

Open Data Science to fight COVID-19: Winning the 500k XPRIZE Pandemic Response Challenge*

No Author Given

No Institute Given

Abstract. During a pandemic, there is a crucial need to predict the number of infections under different scenarios to inform public health, health care and emergency system responses. Given the exponential growth in the number of positive cases and the pressure in the health care systems due to the current COVID-19 pandemic, most countries in the world deployed non-pharmaceutical interventions (NPIs) -such as school closings, restrictions on gatherings and travel controls- designed to reduce human mobility and limit human interactions to contain the spread of the coronavirus. However, such interventions entail significant economic and social costs. Hence, there is a need for principled approaches to both reliably predict the number of confirmed cases under different NPI policies and to recommend NPI regimes that would achieve the optimal balance between their cost and the resulting number of infections. In view of this need, the XPRIZE foundation organized in November of 2020 a four-month global competition called the 500K XPRIZE Pandemic Response Challenge sponsored by Cognizant. It focused on developing data-driven AI models to predict COVID-19 infection rates and prescribe Non-Pharmaceutical Intervention Plans that governments, business leaders and organizations could implement to minimize harm when reopening their economies. In this paper, we describe the deep learning-based COVID-19 predictor and the Pareto-optimal NPI prescriptor developed by the winning team of the competition. In addition, the models were validated in a real-world scenario thanks to an ongoing collaboration with the Valencian Government in Spain. We believe that this experience contributes to the necessary transition to more evidence-driven policy-making, particularly during a pandemic.

Keywords: SARS-CoV-2 · Computational Epidemiology · Data Science for Public Health · Recurrent Neural Networks · Non-Pharmaceutical Interventions · Pareto-front optimization

1 Introduction

During a pandemic, it is of paramount importance to predict the number of infections under different circumstances to inform public health, health care and emergency system responses. Different approaches to predict the evolution of a

* The 500k XPRIZE Pandemic Response Challenge is supported by Cognizant.

pandemic have been proposed in the literature, including traditional compartmental meta-population models –such as SIR or SEIR models [12], complex network models [20], agent-based individual models [10] and purely data-driven time series forecasting models [25].

Given the exponential growth in the number of SARS-CoV-2 infections and the pressure in the health care systems, most countries in the world have implemented non-pharmaceutical interventions (NPIs) during the current coronavirus pandemic, designed to reduce human mobility and limit human interactions to contain the spread of virus. These NPIs range from closing schools and non-essential workplaces to requiring citizens to wear masks and limiting national and/or international travel. How to model the impact that the applied NPIs have on the progression of the pandemic is a non-trivial task, particularly for traditional meta-population approaches. Moreover, the social and economic costs of applying NPIs for a sustained period of time has led to the largest global recession in history, with more than a third of the global population under confinement during the first wave of the pandemic in March - April of 2020. The global GDP shrunk by nearly 22 trillion of US dollars as of January 2021, according to the IMF¹. Beyond the economic cost, the social cost of the pandemic is also staggering, preventing children and teenagers from attending schools, cancelling cultural activities and forbidding people to visit their friends or relatives.

In view of these challenges, the XPRIZE foundation organized in November of 2020 a global competition called the 500K XPRIZE Pandemic Response Challenge sponsored by Cognizant [1]. This four-month challenge focused on the development of data-driven AI systems to *predict* COVID-19 infection rates and *prescribe* Non-pharmaceutical Intervention Plans that governments and communities could implement to minimize harm when reopening their economies.

In this paper, we describe the predictor and prescriptor models developed by the winning team of the competition. The paper is organized as follows: Section 2 provides an overview of the most relevant related work. The data used in the competition is described in Section 3. The predictor and the prescriptor models developed for the Challenge are presented in Section 4 and 5, respectively, followed by the experimental results in Section 6. The main conclusions of our work and our future lines of research are outlined in Section 7.

2 Related work

We built a COVID-19 infections predictor based on Long Short Term Memory (LSTM) networks [13]. Here, we briefly provide an overview of the approaches that are the most similar to ours, *i.e.* based on recurrent neural networks. Comparative analyses with other methods can be found in *e.g.* [2,15,27].

Chatterjee *et al.* [8] applied stacked, bidirectional LSTMs and compared them with multilayer LSTMs. They obtained good accuracy in the prediction of the total number of cases and deaths in the world. Moreover, they did not find any statistical correlation between COVID-19 cases and temperature, sunshine, and precipitation, showing that the number of infections mostly depends on the

¹ <https://www.dw.com/en/coronavirus-global-gdp-to-sink-by-22-trillion-over-covid-says-imf/a-56349323>

behavior and density of the population. In [9], LSTMs were used to predict the evolution of the pandemic in Canada and compared it with the USA, Spain, and Italy. Prompt interventions were found to have a strong impact in minimizing the total number of infections, though the accuracy of their predictions was good only for a relatively short time period. Other examples of early works explored using LSTMs to predict COVID-19 cases and the effect of NPIs in India [4] and Iran [5], with accurate results within a prediction interval of one week up to a month. Clustering algorithms have been used to improve the models' performance. In [21] the authors use an LSTM to predict cases in different states of Brazil. First, they cluster nations by their temporal series of infections and then assign each Brazilian state to the closest cluster. Global COVID-19 case data was also used to cluster countries according to their outcomes in [7,14].

To the best of our knowledge, our work is the first to propose a bank of LSTMs to predict the evolution of the coronavirus pandemic in 236 countries and regions in the world, with good prediction results over a long time period (up to 180 days) and taking into consideration the NPIs applied in each country/region.

Regarding the prescriptor part of our work, there are very few related references. In [26] a multi-objective genetic algorithm was used to find optimal policies using data from Wuhan. Sameni presents an approach to find a balance between interventions and the number of cases with a core compartmental model. This approach requires evaluating the impact of the policy on the evolution of the disease [24]. Several works studied the impact of different NPI policies in the time series of COVID-19 cases, such as [23,22] in Italy, Taiwan and Malaysia. Finally, Miikkulainen *et al.* propose a neuroevolution approach to identify a Pareto-optimal set of NPIs [18]. Note that this approach was recommended during the XPRIZE Challenge, as it was organized in collaboration with Cognizant and the authors of [18] are affiliated with it.

3 Data

The coronavirus is the first global pandemic for which there is extensive data captured and shared on a daily basis for most countries and regions in the world. The Challenge leveraged publicly available official COVID-19 case data together with the Oxford COVID-19 Government Response Tracker data set² as the main data sources to be used during the competition [11]. This data set provides information for 186 countries and state/region-level data for the US, UK, Canada, and Brazil. In the Challenge, 182 countries³, the 50 US states and the 4 regions in the UK were considered, yielding a total of 236 countries or regions.

The available data sources can be split into *case*-related data, *i.e.* number of daily confirmed COVID-19 cases, and *action or NPI*-related data, *i.e.* the NPIs and their level of activation each day for each country/region. In the Challenge, we considered 12 NPIs of two types: *confinement-based* and *public health-based*. Table 1 summarizes all the considered NPIs and their possible levels of activation. The meaning of each NPI can be found in the Supplementary material.

² <https://www.bsg.ox.ac.uk/research/research-projects/coronavirus-government-response-tracker>

³ Tonga, Malta, Turkmenistan y Virgin Islands- were not considered due to lack of reliable data.

Table 1. NPIs considered in the Challenge. The predictor is trained with confinement interventions (C1 to C8). Both confinement and public health interventions are considered in the prescriptor.

NPI name	Activation values
Confinement Interventions	
C1. School closing	[0,1,2,3]
C2. Workplace closing	[0,1,2,3]
C3. Cancel public events	[0,1,2]
C4. Restrictions on gatherings	[0,1,2,3]
C5. Close public transport	[0,1,2]
C6. Stay at home requirements	[0,1,2,3]
C7. Restrictions on internal movement	[0,1,2]
C8. International travel controls	[0,1,2,3]
Public Health Interventions	
H1. Public information campaigns	[0,1,2]
H2. Testing policy	[0,1,2,3]
H3. Contact tracing	[0,1,2]
H6. Facial coverings	[0,1,2,3,4]

4 Predictors of COVID-19 cases

This part of the Challenge required building a predictor of the number of confirmed COVID-19 cases in the 236 countries and regions considered for up to 180 days into the future, and taking into consideration the different NPIs implemented in each country/region. Evidently, the NPIs should impact the transmission of the disease and hence in the number of cases. Next, we summarize our notation, followed by a description of our deep learning-based predictive model.

4.1 Notation

In the following, we will use the following terms and notation:

- 1. GEO:** We denote as GEO a country or a region (*e.g.* California). We use the index j to refer to each GEO.
- 2. Population (P^j):** P^j denotes the total population of GEO j . We assume that each GEO's population is constant during the entire period of time.
- 3. NewCases (X_n^j):** The daily number of new cases on day n and GEO j is denoted by X_n^j . The first day considered is March, 11th 2020.
- 4. ConfirmedCases (Y_n^j):** The cumulative number of confirmed cases up to day n in GEO j is given by $Y_n^j = \sum_{i=1}^n X_i^j$.
- 5. SmoothedNewCases (Z_n^j):** We compute the average number of new cases between days $n - K + 1$ and n in GEO j as $Z_n^j = \frac{1}{K} \sum_{i=0}^{K-1} X_{n-i}^j$. This prevents noise due to different imputation policies (some GEOs do not report cases on weekends, while others do). We use $K = 7$ to smooth over one week.
- 6. CaseRatio (C_n^j):** The ratio of cases between two consecutive days is denoted by $C_n^j = Z_n^j / Z_{n-1}^j$. It indicates the growth/decrease in the number of cases.

7. Susceptible Population (S_n^j): The number of susceptible individuals to be infected with coronavirus on day n and for GEO j is denoted by S_n^j .

8. ScaledCaseRatio (R_n^j): It is the CaseRatio C_n^j divided by the proportion of susceptible individuals in GEO j , $R_n^j = C_n^j \frac{P_j}{S_n^j}$. It captures the effects of a finite population, as it depends on proportion of susceptible individuals in GEO j .

9. Action (A_n^j): The vector with the applied NPIs in GEO j on day n .

10. Stringency of A_n^j ($Str_{A_n^j}^j$): The stringency of an NPI applied in GEO j on day n is given by $Str_{A_n^j}^j = \sum_{i=C1}^{H6} a_n^j(i) \cdot Cost^j(i)$, where $Cost^j$ is the cost vector of each of the 12 different types of NPIs ([C1...C8,H1,H2,H3,H6]) in GEO j .

11. Intervention Policy (IP): The sequence of daily 12-dimensional NPI or action vectors applied over a time period T .

12. Stringency of an Intervention Policy: The sum of the stringencies of the NPIs or actions A_n^j applied each day n over the time period T .

We denote estimations with a $\hat{\cdot}$ symbol, *e.g.* \hat{X}_n^j is the estimated number new cases and \hat{R}_n^j the estimated scaled case ratio, both for GEO j and day n .

4.2 SIR Epidemiological Model

The predictors model the dynamics of the epidemics in each GEO j using an underlying basic SIR compartmental meta-population model [3]. In this model, the population is divided into three different states: S (Susceptible), Z (Infected), and D (Removed, due to recovery or death). The dynamics of such an SIR model are presented in the Supplementary material. The evolution of the number of infected individuals is given by $\frac{dZ^j}{dt} = \beta \frac{S^j}{P_j} Z^j - \mu Z^j$, where β is the infection rate which controls the probability of transition between the S and Z ; and μ is the recovery or removal rate, controlling the probability of transition between the Z and D states. When discretizing $\frac{dZ^j}{dt}$ for two consecutive days, we obtain

$$Z_n^j = Z_{n-1}^j + \beta \frac{S_{n-1}^j}{P_j} Z_{n-1}^j - \mu Z_{n-1}^j = \left(1 + \beta \frac{S_{n-1}^j}{P_j} - \mu\right) Z_{n-1}^j. \quad (1)$$

which yields

$$R_n^j = \frac{(1 - \mu)P_j}{S_n^j} + \beta = \frac{Z_n^j}{Z_{n-1}^j} \frac{P_j}{S_n^j}. \quad (2)$$

This equation links R_n^j with the parameters of the SIR model. The larger the R_n^j , the larger $\frac{Z_n^j}{Z_{n-1}^j}$ and hence the larger the growth in the number of cases. Given that μ is constant in (2), the larger the infection rate β , the larger the R_n^j . Moreover, the infection rate and thus R_n^j depend on the applied NPIs.

If we predict \hat{R}_n^j , we can estimate the number of cases for day n at GEO j :

$$\hat{X}_n^j = \left(\hat{R}_n^j \frac{S_{n-1}^j}{P_j} - 1 \right) K Z_{n-1}^j + X_{n-K}^j. \quad (3)$$

where $K = 7$ is the size of the temporal window used to compute Z_n . As previously explained, X_{n-K} is the reported new cases for day $n - K$; \hat{R}_n^j is the

predicted R_n^j ; P^j is the population of GEO j ; and Z_{n-1}^j is the cumulative number of cases averaged over K days for day $n-1$ in GEO j .

Thus, the goal of the predictors is to estimate \hat{R}_n^j given the data up to day $n-1$. Since R_n^j depends on the transmission rate and the dependency of the transmission rate on the NPIs, the predictors consider the number of COVID-19 infections (*context*) and the applied NPIs (*actions*) each day in each GEO.

4.3 Baseline or standard predictor

The baseline or standard predictor was provided by the Challenge organizers [18]. It consists of two parallel LSTMs, one to model the *context* – given by the R_n^j – and the other to model the *actions* (A_n^j) applied on day n in GEO j . Figure 1 (left) depicts the architecture of this baseline model. It uses the context and action data to get predictions separately, joining both outputs via a lambda merge layer. The lambda layer combines the output of the context LSTM h

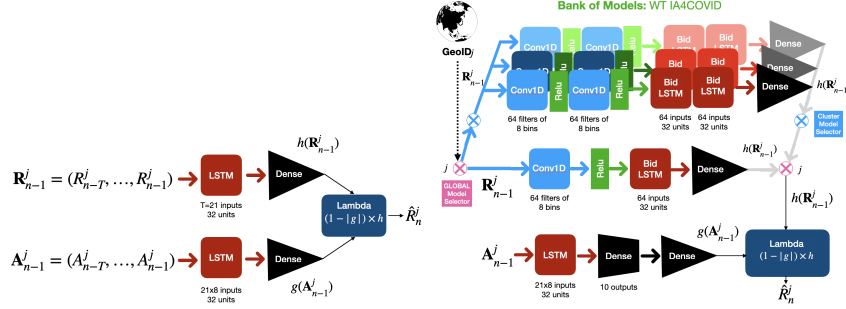


Fig. 1. Left: Baseline LSTM-based Predictor; Right: WT predictor architecture.

(top) and the output of the action LSTM g (down), represented in Figure 1. The input to the LSTM h is the vector of values of R_n in the previous T days in GEO j , namely $\mathbf{R}_{n-1}^j = (R_{n-T}^j, \dots, R_{n-1}^j)$. The input to the LSTM g is the matrix of 12-dimensional NPIs (actions) taken during the previous T days in GEO j , namely $\mathbf{A}_{n-1}^j = (A_{n-T}^j, \dots, A_{n-1}^j)$.

In our experiments we set $T = 21$, similarly to [18]. Such time window mitigates the noise due to how different GEOs report cases (*e.g.* Spain does not report confirmed cases during the weekends and holidays, France reports just four days per week, etc.). Moreover, this temporal granularity enables the model to consider the average period of 12-15 days between being exposed to the coronavirus, being detected and tested as a new confirmed case [16].

The output of the lambda layer for day n is the predicted \hat{R}_n^j given by

$$\hat{R}_n^j = f(\mathbf{A}_{n-1}^j, \mathbf{R}_{n-1}^j) = (1 - g(\mathbf{A}_{n-1}^j))h(\mathbf{R}_{n-1}^j) \quad (4)$$

with $g(\mathbf{A}_{n-1}^j) \in [0, 1]$ and $h(\mathbf{R}_{n-1}^j) \geq 0$. More details about the baseline model can be found in [18]. Note that when making predictions into the future, the

R_{n-i}^j values in the vector \mathbf{R}_n^j are replaced by the estimations provided by the predictor, namely \hat{R}_{n-i}^j , for $n-i > \text{today}$, $i = 1, \dots, T$.

4.4 WT predictor

Similarly to the baseline predictor, we implemented an architecture with 2 LSTM-based branches: a *context* branch, where we modeled the R_n time series and an *action* branch, where we modeled the time series of the eight confinement-based ([C1...C8]) Non-pharmaceutical Interventions. While we did not consider public health-based NPIs, we improved the baseline predictor in several ways. In the following, we refer to this improved model as WT predictor.

4.4.1. Context branch

We identified large variability in the time series of confirmed COVID-19 cases for the different GEOs, which made it difficult for a single LSTM *context* model to perform well everywhere. More precisely, the analysis of the weights of a single model trained on all the data showed that the LSTM matrices were full rank. Hence, we opted for a solution that included a bank of LSTM context models, as shown in Figure 1 (right).

Bank of context models We created the bank as follows: First, we clustered the GEOs via a K-means algorithm applied to the time series of reported number of COVID-19 cases per 100K inhabitants. We optimized the number of clusters using the Elbow method, obtaining 15 different clusters shown in the Supplementary material.

Next, we trained a *reference* LSTM model with data from the 20 most-affected GEOs and 15 different *cluster* LSTM models using data from all the GEOs in each of the 15 clusters. In our experiments, we set March 11th, 2020 as the starting date for training the models. We then evaluated the reference and all the cluster models on our testing data for all the GEOs. Our testing period started on Nov. 1st for long-term evaluation and Dec. 1st for short-term evaluation, ending on Dec. 21st, 2020. We automatically selected the model with the lowest MAE per 100K inhabitants in each GEO, applying Occam’s razor principle to minimize the number of models in our bank. Thus, we favored the *reference* model when it obtained a similar performance to the best of the cluster models. As a result of this process, we selected nine models to be used in the Challenge: the *reference* model, applied in 135 GEOs; and eight *cluster* models applied in the remaining GEOs. A visualization of the cluster and model assignments can be found here⁴.

LSTMs Architecture. In the context branch (*h*) we implemented two different LSTM-based architectures, as depicted in Figure 1 (right), one for the *reference* model and the other for each of the eight *cluster* models. The *reference* model includes a convolutional layer, a ReLu layer as the activation function for the outputs of the CNN, and a bidirectional LSTM followed by a dense layer. Each convolutional layer has 64 filters of size 8. This reference model empirically generalized well for 135 GEOs.

The *cluster* models consist of a stacked version of the architecture of the reference model, with two convolutional layers and two stacked bidirectional

⁴ Anonymized due to double-blind submission.

LSTMs. Each convolutional layer also has 64 filters of size 8. We use a ReLu layer as the activation function for the outputs of the CNNs and add a final dense layer. After the double 1D convolution spans the characterization of the input sequence, the first LSTM encodes such a characterization in states of 64 dimensions (bidirectional) and feeds into the second LSTM, whose units can now operate at a different time scale. This added complexity enabled the models to perform well in the GEOs where the reference model did not. After model selection, we obtained a bank of eight different cluster models.

4.4.2. Action branch

We used an LSTM followed by two dense layers to smooth the output and hence better capture non-linearities. Similarly to [18], we used a sigmoid activation function to guarantee that the action layer’s output to be in $[0,1]$. Since increasing the activation or stringency of an NPI should not decrease its effectiveness, g is constrained to satisfy the condition: if $\min(A - A') \geq 0 \rightarrow g(A) \geq g(A')$. This constraint is enforced by setting all trainable parameters of g to be non-negative (absolute value) after each parameter update. Note that convolution here is not considered in order to keep the raw NPI constraints. The WT predictor only considers the confinement NPIs, so each A_n^i is an 8-dimensional vector with the level of activation of the eight confinement NPIs (see Table 1).

4.4.3. Merge function

The two branches use the data from the last 21 days that are combined into a final dense layer to get the predicted \hat{R}_n . The outputs of each branch (h and g) are merged by the lambda function defined in (4). Thus, the predicted \hat{R}_n provided by the *context* branch is modified by the output from the *action* branch. The stricter the NPIs, the larger the output from the action layer, thus reducing the context layer’s output. Finally, once the model gives the predicted \hat{R}_n , the predicted number of new infections for day n , \hat{X}_n , is obtained using (3).

5 Prescriptor model

The final phase of the XPRIZE competition required building a *prescriptor* which would recommend for each GEO and for any period of time, up to 10 different Intervention Policies (IP) with the best balance between their economic/social cost and the resulting number of COVID-19 cases.

Thus, it entailed solving a two-objective optimization problem by identifying the set of solutions that would be on the Pareto front [6,17,18,19]. On the one hand, there is the *stringency* of a certain IP which captured the sum of the costs of implementing such a policy. On the other hand, there is the number of COVID-19 cases per 100K inhabitants which would result from applying such IP. Given that this is a hypothetical scenario, the number of COVID-19 infections under the IPs was estimated by the *baseline* or standard predictor provided by the XPRIZE Challenge organizers. All the teams used the same predictor to enable the judges to compare the prescriptors from different teams properly.

Our goal in the Prescription phase of the competition was to develop an *interpretable*, data-driven and flexible prescription framework that would be usable by non machine-learning experts, such as citizens and policymakers in the Va-

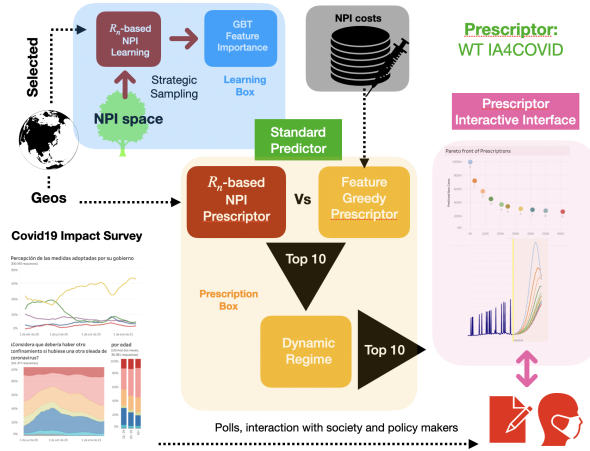


Fig. 2. WT Prescriptor. The (offline) learning box (in blue) infers the convergence \hat{R}_n for the sampled NPIs, and the Gradient Boosted Trees identify the feature importance. The prescriptor relies on the standard XPRIZE predictor. The first set of NPIs is obtained given by the NPI- \hat{R}_n mapping. The second set is obtained via a feature importance-based greedy algorithm. These two sets compete and up to 10 non-dominated IPs are selected.

lencian Government. Our design principles were therefore driven by developing explainable and transparent models.

The Challenge entailed finding the set of Pareto-optimal IPs with the best trade-off between their economic/social costs and their associated number of resulting COVID-19 cases. An intervention policy IP_1 **dominates** another intervention policy IP_2 if the stringency(IP_1) \leq stringency(IP_2) and the resulting number of COVID-19 cases under IP_1 $<$ than under IP_2 . The goal was to find up to 10 IPs for each GEO, for any time period and any costs that would dominate the rest of possible intervention policies. As in the case of our predictor, we decided to combine complementary approaches to have a more robust solution, depicted in Figure 2.

5.1 Modeling the NPI - COVID-19 cases space

Before building the prescriptor, we performed an exploratory data analysis of the problem space. Our goal was to shed light on the relationship between the NPIs and the resulting number of COVID-19 cases. Considering all the possible values of each dimension of the NPI or action vector, there are 7,776,000 possible combinations of NPI vectors that could be applied at each time step.

Each NPI vector, when applied for a minimum amount of time, would lead to a reduction or increase in the number of COVID-19 cases in the GEO where it is applied (see Equation 4). To better understand the impact that different NPI vectors have on the number of COVID-19 cases, we ran numerous experiments where we called the predictor with different values of the NPI vector over varying time periods of 30 to 90 days and on a sample of 21 representative GEOs from

different continents⁵, namely: United States, Brazil, India, Mexico, Italy, China, United Kingdom, France, England, Russia, Iran, Spain, Argentina, Colombia, New York State, Peru, Germany, Poland, South Africa, Texas and California. For each case, we obtained the resulting \hat{R}_n estimated by the predictor.

In our experiments, we observed that the **same NPI vector** would lead to the **same convergence \hat{R}_n** in **all the GEOs** and over **any time period** provided that the NPI was applied for long enough (see a justification in the Supplementary material). Moreover, we found that the convergence time of \hat{R}_n is inversely proportional to its value. As per Eq. (2), note that the larger the \hat{R}_n , the larger the number of resulting COVID-19 cases. We refer to this finding as the *R_n synchronization principle*. Moreover, all countries underwent a transitory period of ≈ 21 days since the application of a certain NPI before their \hat{R}_n started converging towards its convergence value. Figure 3 illustrates the convergence of the \hat{R}_n for two different NPI vectors in the 21 selected GEOs.

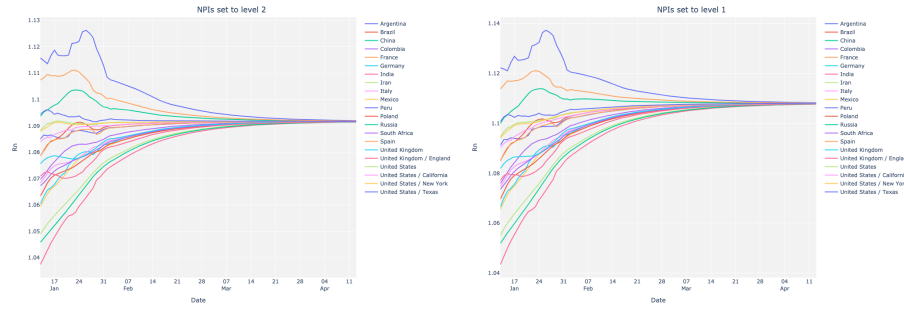


Fig. 3. \hat{R}_n convergence for two different NPI vectors on 21 representative GEOs.

5.2 Prescriptor method 1: R_n -based NPI selection

Based on the *R_n synchronization principle*, one could easily obtain the Pareto-optimal front of intervention policies if the mapping between the 7.8 million of possible combinations of the NPI vector and their associated convergence \hat{R}_n were to be known. Unfortunately, generating such a mapping was not feasible in the time frame provided by the Challenge as it would require making millions of calls to the predict function. Hence, we opted for computing a sample of such a matrix, obtained as (1) all the NPI vectors with stringencies [0 to 6] and [28 to 34]; (2) all NPI vectors with one and two non-zero entries; and (3) a random sample of 10,000 NPIs.

In addition to the convergence \hat{R}_n , we computed the total number of cases in 20 and 60 days. The distribution of the sample of NPI vectors is shown in the Supplementary material.

Using this NPI- \hat{R}_n matrix, we trained state-of-the-art machine-learning models to predict the \hat{R}_n for any given NPI vector. The best performing and explainable model were Gradient Boosted Trees, which obtained a MAE on the test set

⁵ We selected amongst the most affected countries and regions across the globe.

of 0.0003. While such MAE was still too large for us to be able to fill-in all the missing elements in the NPI- \hat{R}_n matrix, we carried out a feature importance analysis and discovered that the C2, C1, H2, C4 and C5 interventions are, in this order, the most important to predict their associated \hat{R}_n and hence the resulting number of COVID-19 cases (see Supplementary material for details).

Thus, we also included in our NPI- \hat{R}_n matrix all the NPI vectors with non-zero values in their C1, C2, C4, C5 and H2 interventions and zero in the rest of the dimensions. This led to a total of 54,652 NPI vectors. As a result, we generated a matrix with the mapping between these different NPI vectors, their associated stringencies (at cost 1), the number of cases that they would lead to at 20 days and at 60 days, and their convergence \hat{R}_n . We carried out all computations on the sample of 21 previously listed GEOs.

At run time, given an input cost vector, the prescriptor computes the stringency of each row in the NPI- \hat{R}_n matrix and identifies the NPI combinations that are on the Pareto front by selecting those that lead to the best trade-off between their stringencies, their associated number of cases at 20 and 60 days and their convergence \hat{R}_n . More details are included in the Supplementary material.

5.3 Prescriptor method 2: Feature greedy NPI selection

As per the feature importance analysis described above and given a cost vector, we developed a greedy NPI prescriptor as follows: each dimension of the NPI vector is ranked by its *priority*, computed as its feature importance divided by its cost. This prescriptor consists of a greedy algorithm that consecutively activates to its maximum value each NPI dimension by order of its priority. This method is related to the greedy strategies developed to solve the knapsack problem⁶.

5.4 Prescriptor combination

Each of the methods above provides a set of NPI recommendations for each GEO for each day. From such a set, we select the 10 best NPIs that satisfy the following criteria: (1) they are not dominated by any other NPI; and (2) they contribute to having a diverse set of NPIs that cover the full range of possible stringency values. Additional details are included in the Supplementary Material.

5.5 Intervention policy definition

Finally, the prescriptor needs to provide a set of up to 10 Intervention Policies, *i.e.* *dynamic* regimes of applying the selected NPIs over the time period of interest. To do so, we compute all possible combinations of subsequently applying the selected NPIs in chunks of minimum 14 days (to enable the NPIs to act) and identify the Pareto-front set of combinations that would yield the optimal trade-off between stringency and number of cases. The total number of chunks is dynamically determined. From this set of combinations, we again select the 10 that (1) are not dominated by any other policy; (2) contribute to having a diverse set of policies along the stringency axis and (3) minimize the changes in NPIs, as every NPI change has a social cost from a practical perspective.

⁶ See https://en.wikipedia.org/wiki/Knapsack_problem.

Two screenshots of the interactive visualization that we developed so policy-makers could easily access and compare the prescribed IPs are shown in the Supplementary Material and can be found here⁷.

6 Experimental results

In this Section, we report the results of quantitatively evaluating our predictor both in short and long-term prediction scenarios and qualitatively assessing the performance of our predictor and prescriptor in hypothetical scenarios.

6.1 Predictor

We evaluated the predictive performance of our COVID-19 cases predictor and compared it to the baseline model under different scenarios. We computed both the Mean Absolute Error (MAE) of the estimated number of COVID-19 cases per 100K inhabitants for each GEO in the Challenge and the Mean Rank of our model when compared to the baseline model.

All the models were trained with data from the Oxford COVID-19 Government Response Tracker dataset, from March 11th to December 17th 2020, for the 20 most affected countries in terms of confirmed deaths. As the consistency of the model is an important characteristic to assess, we evaluated the models both in short-term and long-term predictions. Short-term evaluations consisted in generating predictions for 3 weeks ahead into the future for the time period between Dec 1st and Dec 21st, 2020. Long-term evaluations were two-fold: (1) First, with historic data, we tested the predictions between Nov 1st and Dec 21st, 2020; (2) Second, we ran the predictors under three different 180-day prediction scenarios: (i) a scenario where the NPIs were frozen as of their values in Dec 21st 2020; (ii) a scenario with all NPIs in all GEOs were set to their maximum levels; and (iii) a scenario where all NPIs in all GEOs were set to 0. The behavior of our model under these three conditions made intuitive sense, as depicted in Figure 4.

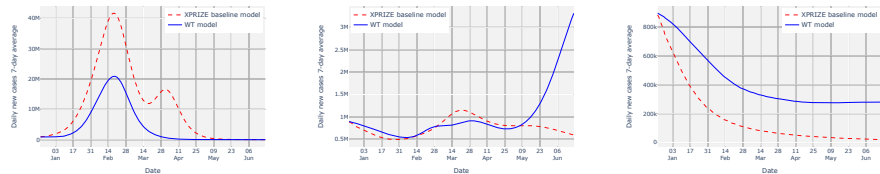


Fig. 4. Smoothed predicted daily new cases worldwide (7-day average) for three different future scenarios based on three different IPs: zero (left), frozen (center) and maximal (right) NPIs applied.

Table 2 displays the MAE per 100K inhabitants and the Mean Rank of the proposed model when compared to the baseline model provided by the XPRIZE

⁷ Anonymized due to double-blind submission.

Table 2. Predictor results.

Predictor	Short-term		Long-term	
	MAE	Mean Rank	MAE	Mean Rank
XPRIZE LSTM baseline	157.924142	2.106383	935.340780	2.297872
WT (w/o clusters)	138.208982	2.144681	825.375377	1.834043
WT with clusters	126.331216	1.748936	803.587381	1.868085

organizers. We also include the results of only using our *reference* context model without the clusters. As seen on the Table, our model outperforms the baseline model in all evaluation scenarios in terms of MAE and Mean Rank. Moreover, during the predictor evaluation phase of the XPRIZE Challenge, our predictor ranked third in the world in Mean Rank amongst all the teams, first in Mean Rank in Asian and in European GEOs.

As per our collaboration with the President of the Valencian Government in Spain, we were able to share the predictions of our predictor during the 3rd wave of the COVID-19 pandemic that started right after Christmas of 2020. Figure 5 shows the predictions of our model (blue) when compared to the baseline predictor (red) and the ground truth (yellow). As seen in the Figure, our predictor was very accurate in predicting the evolution of the pandemic while taking into account the different NPIs that were implemented at the time. It provided valuable input to the Government in their decision-making.

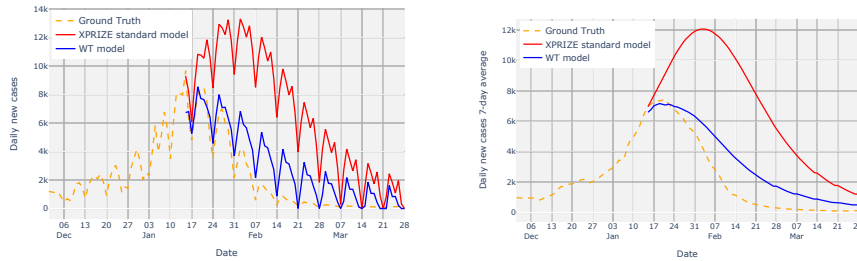


Fig. 5. Predictions for the Valencian region (Spain) during the third wave: daily new cases (left) and smoothed daily new cases (right).

6.2 Speed and Resource Use

In terms of training, we used an Intel Core i7 with 256 Gb RAM and GPU. The training time of the *reference* model with 20 trials was 108 minutes and of the *cluster* models ranged between 24 minutes (largest cluster with 106 GEOs) and 44 seconds (smallest cluster with 2 GEOs).

We carried out our prediction experiments on an Intel Core i7, 4 cores, 2,7 Ghz, 16GB 2133MHz LPDDR3. Table 3 summarizes the times needed to produce a prediction for all the GEOs by the baseline model and our proposed model for three different sizes of the prediction period. As seen on the Table, the

computation needs of our model were well below the maximum time allowed in the XPRIZE competition (60 minutes). We favored simplicity in our design and aimed to minimize the energy consumption to be as planet-friendly as possible.

Table 3. Total time needed to generate predictions for all the GEOs.

Predictor	Window size of prediction		
	31-days	61-days	180-days
Baseline	212 seconds	409 seconds	1,092 seconds
WT	417 seconds	597 seconds	1,239 seconds

6.3 Prescriptor

Given the hypothetical nature of the prescriptor, we were not able to quantitatively evaluate its performance against ground truth. However, we did carry out domination tests between the IPs recommended by our model when compared to a greedy algorithm for the 236 GEOs in the Challenge and under both unitary and random costs policies for a time period of 60 days into the future. Figure 6 depicts the recommended IPs by our model (orange and green) when compared to a greedy prescriptor (blue). Table 4 shows the number of times the IPs recommended by the WT prescriptor dominated and were dominated by the IPs suggested by the greedy approach for all GEOs. Moreover, our prescriptor provided the IP recommendations in under 2 hours for all GEOs in the Challenge, well below the maximum allowed limit of 6 hours.

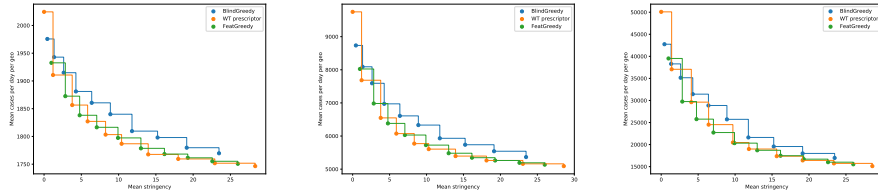


Fig. 6. Number of cases vs stringency obtained from prescriptions generated for 5 days (left), 31 days (center) and 90 days (right).

7 Conclusions and Future Work

In this paper, we have described the models developed by the winning team of the 500K XPRIZE Pandemic Response Challenge. The competition entailed first developing a model to predict the number of COVID-19 cases in 236 countries/regions in the world, for up to 180 days into the future and considering the Non-pharmaceutical Interventions deployed in each country/region. In this phase, we developed an LSTM-based bank of models which outperformed the baseline model provided by the Challenge organizers and yielded the third best Mean Rank amongst all the teams in the competition. The proposed model was

Table 4. Prescriptor results: # of dominating / # of dominated prescriptions for 5-day (from Aug 1st to Aug 5th, 2020), 31-day (from Jan 1st to Jan 31st, 2021) and 90-day (from Jan 1st to Mar 31st, 2021) time periods.

Prescriptor	Window size of prescription		
	5-days	31-days	90-days
Greedy	127 / 1814	130 / 1829	163 / 1839
Feature greedy	921 / 114	930 / 117	986 / 163
WT prescriptor	927 / 47	934 / 48	986 / 137

successfully used by the President of the Valencian government in Spain during the third wave of COVID-19 infections in December - February 2021.

Next, the teams were asked to develop a prescription model that would recommend up to 10 Intervention Policies in each of the 236 countries/regions in the world for any time period and costs that would achieve the best trade-off between the total cost of the IP and the resulting number of coronavirus infections. Our winning solution leveraged the R_n *synchronization principle* to provide Pareto-optimal Intervention Policies that clearly dominated other approaches.

We believe that this work contributes to the necessary transition to more evidence-driven policy-making, particularly during a pandemic. Future lines of work include developing the intervention prescriptor within the Valencian Government, developing a theoretical proof of the R_n synchronization principle and including the impact of vaccinations in our model.

References

1. 500k XPRIZE Pandemic Response Challenge, sponsored by Cognizant, <https://www.xprize.org/challenge/pandemicresponse>
2. Alakus, T., Turkoglu, I.: Comparison of deep learning approaches to predict COVID-19 infection. *Chaos, Solitons & Fractals* **140**, 110120 (2020)
3. Allen, L.: Some discrete-time SI, SIR, and SIS epidemic models. *Math. Biosci.* **124**(1), 83–105 (1994)
4. Arora, P., Kumar, H., Panigrahi, B.K.: Prediction and analysis of covid-19 positive cases using deep learning models: A descriptive case study of india. *Chaos, Solitons & Fractals* **139**, 110017 (2020)
5. Ayyoubzadeh, S., Ayyoubzadeh, S., Zahedi, H., Ahmadi, M., Kalhori, S.: Predicting COVID-19 incidence through analysis of Google trends data in Iran: data mining and deep learning pilot study. *JMIR Public Health Surveill.* **6**(2) (2020)
6. Belakaria, S., Deshwal, A., Doppa, J.: Max-value entropy search for multi-objective bayesian optimization. In: Wallach, H., Larochelle, H., Beygelzimer, A., d'Alché-Buc, F., Fox, E., Garnett, R. (eds.) *NeurIPS*. vol. 32 (2019)
7. Carrillo-Larco, R.M., Castillo-Cara, M.: Using country-level variables to classify countries according to the number of confirmed covid-19 cases: An unsupervised machine learning approach. *Wellcome Open Res.* **5** (2020)
8. Chatterjee, A., Gerdes, M., Martinez, S.: Statistical explorations and univariate timeseries analysis on COVID-19 datasets to understand the trend of disease spreading and death. *Sensors* **20**(11), 3089 (2020)

9. Chimmula, V.K.R., Zhang, L.: Time series forecasting of covid-19 transmission in canada using lstm networks. *Chaos, Solitons & Fractals* **135**, 109864 (2020)
10. Ferguson, N., Cummings, D., Cauchemez, S., Fraser, C., *et al*: Strategies for containing an emerging influenza pandemic in Southeast Asia. *Nature* **437**(7056), 209–214 (2005)
11. Hale, T., Angrist, N., Goldszmidt, R., Kira, B., *et al.*: A global panel database of pandemic policies (Oxford COVID-19 Government Response Tracker). *Nat. Hum. Behav.* pp. 1–10 (2021)
12. Hethcote, H.: The mathematics of infectious diseases. *SIAM Rev.* **42**(4), 599–653 (2000)
13. Hochreiter, S., Schmidhuber, J.: Long short-term memory. *Neural Comput.* **9**(8), 1735–1780 (1997)
14. Khan, M., Hossain, A.: Machine learning approaches reveal that the number of tests do not matter to the prediction of global confirmed COVID-19 cases. *Front. Artif. Intell. Appl.* **3**, 90 (2020). <https://doi.org/10.3389/frai.2020.561801>
15. Kırbaş, I., Sözen, A., Tuncer, A., Kazancıoğlu, F.Ş.: Comparative analysis and forecasting of COVID-19 cases in various european countries with ARIMA, NARNN and LSTM approaches. *Chaos, Solitons & Fractals* **138** (2020)
16. Lauer, S., Grantz, K., Bi, Q., Jones, F., *et al*: The incubation period of coronavirus disease 2019 (COVID-19) from publicly reported confirmed cases: estimation and application. *Ann. Intern. Med.* **172**(9), 577–582 (2020)
17. Lu, Z., Whalen, I., Dhebar, Y., Deb, K., *et al.*: NSGA-Net: Neural architecture search using multi-objective genetic algorithm (extended abstract). In: Bessiere, C. (ed.) *Proc. of the 29th International Joint Conference on Artificial Intelligence, IJCAI-20*. pp. 4750–4754 (7 2020)
18. Miikkulainen, R., Francon, O., Meyerson, E., Qiu, X., *et al.*: From prediction to prescription: Evolutionary optimization of nonpharmaceutical interventions in the COVID-19 pandemic. *IEEE Trans. Evol. Comput.* **25**(2), 386–401 (2021)
19. Navon, A., Shamsian, A., Chechik, G., Fetaya, E.: Learning the pareto front with hypernetworks. In: *Int. Conf. on Learning Representations* (2021)
20. Pastor-Satorras, R., Castellano, C., Van Mieghem, P., Vespignani, A.: Epidemic processes in complex networks. *Rev. Mod. Phys.* **87**, 925–979 (Aug 2015)
21. Pereira, I., Guerin, J., Silva J., A.G., Garcia, G., Piscitelli, P., Miani, A., Distante, C., Gonçalves, L.: Forecasting covid-19 dynamics in brazil: a data driven approach. *Int. J. Environ. Res. Public Health* **17**(14), 5115 (2020)
22. Rahman, M., Zaman, N., Asyhari, A., Al-Turjman, F., *et al*: Data-driven dynamic clustering framework for mitigating the adverse economic impact of COVID-19 lockdown practices. *Sustain. Cities Socy* **62**, 102372 (2020)
23. Riccardi, A., Gemignani, J., Fernández-Navarro, F., Heffernan, A.: Optimisation of non-pharmaceutical measures in COVID-19 growth via neural networks. *IEEE Trans. Emerg. Topics Comput.* **5**(1), 79–91 (2021)
24. Sameni, R.: Model-based prediction and optimal control of pandemics by nonpharmaceutical interventions. *arXiv preprint arXiv:2102.06609* (2021)
25. Tayarani, N., Mohammad, H.: Applications of artificial intelligence in battling against COVID-19: A literature review. *Chaos, Solitons & Fractals* p. 110338 (2020)
26. Yousefpour, A., Jahanshahi, H., Bekiros, S.: Optimal policies for control of the novel coronavirus disease outbreak. *Chaos, Solitons & Fractals* **136** (2020)
27. Zeroual, A., Harrou, F., Dairi, A., Sun, Y.: Deep learning methods for forecasting COVID-19 time-series data: A comparative study. *Chaos, Solitons & Fractals* **140** (2020)

Supplementary Material

No Author Given

No Institute Given

A Non-Pharmaceutical Interventions

Table 1 summarizes the NPIs considered in the Challenge, their meanings and possible levels of activation.

Table 1: NPIs considered in the Challenge. The predictor is trained with confinement interventions (C1 to C8). Both confinement and public health interventions are considered in the prescriptor.

NPI name	Level 0	Level 1	Level 2	Level 3	Level 4
Confinement Interventions					
C1. School closing	Nothing	Recommend closing	Partial closing (e.g. just high school, or just public schools)	Complete closing	
C2. Workplace closing	Nothing	Recommend closing (or work from home)	Require closing (or work from home) for some sectors/categories of workers	Require closing (or work from home) all-but-essential workplaces	
C3. Cancel public events	Nothing	Recommend cancelling	Require cancelling		
C4. Restrictions on gatherings	Nothing	Cancel very large gatherings (above 1000 people)	Cancel gatherings between 101-1000 people	Cancel gatherings between 11-100 people	Cancel gatherings of 10 or less people
C5. Close public transport	Nothing	Recommend closing (or significantly reduce volume, routes and/or means of transport available)	Require closing (or prohibit most citizens from using it)		
C6. Stay at home requirements	Nothing	Recommend not leaving home	Require not leaving house with exceptions for daily exercise, grocery shopping, and <i>essential</i> trips	Require not leaving house with minimal exceptions (e.g. allowed to leave once a week, or only one person can leave at a time, etc)	
C7. Restrictions on internal movement	Nothing	Recommend not to travel between regions/cities	Internal movement restrictions in place		
C8. International travel controls	Nothing	Screening arrivals	Quarantine arrivals from some or all regions	Banning on arrivals from some regions	

NPI name	Level 0	Level 1	Level 2	Level 3	Level 4
Public Health Interventions					
H1. Public information campaigns	No COVID-19 public information campaigns	Public officials urging caution about COVID-19	Coordinated public information campaign (e.g. across traditional and social media)		
H2. Testing policy	No testing policy	Only those who both (a) have symptoms AND (b) meet specific criteria (e.g. key workers, admitted to hospital, came into contact with a known case, returned from overseas)	Testing of anyone showing COVID-19 symptoms	Open public testing (e.g. "drive through" testing available to asymptomatic people)	
H3. Contact tracing	No contact tracing	Limited contact tracing; not done for all cases	Comprehensive contact tracing; done for all identified cases		
H6. Facial coverings	No policy	Recommended	Required in some specified shared/public spaces outside the home with other people present, or some situations when social distancing not possible	Required in all shared/public spaces outside the home with other people present or all situations when social distancing not possible	Required outside the home at all times regardless of location or presence of other people

B SIR Epidemiological Model

The predictors model the dynamics of the epidemics in each GEO j using a basic SIR compartmental meta-population model [1,2]. In this model, the population is divided into three different states: S (Susceptible), Z (Infected), and D (Removed, due to recovery or death). The dynamics of such an SIR model is given by the following set of differential equations:

$$\begin{aligned}
\frac{dS^j}{dt} &= -\beta \frac{S^j}{P_j} Z^j \\
\frac{dZ^j}{dt} &= \beta \frac{S^j}{P_j} Z^j - \mu Z^j \\
\frac{dD^j}{dt} &= \mu Z^j
\end{aligned} \tag{1}$$

where β is the infection rate which controls the probability of transition between the S and Z ; and μ is the recovery or removal rate, controlling the probability of

transition between the Z and D states. Previous work [9] has estimated $\mu = 0.08$ for SARS-CoV-2.

When discretizing $\frac{dZ^j}{dt}$ for two consecutive days, we get

$$Z_n^j = Z_{n-1}^j + \beta \frac{S_{n-1}^j}{P_j} Z_{n-1}^j - \mu Z_{n-1}^j = \left(1 + \beta \frac{S_{n-1}^j}{P_j} - \mu \right) Z_{n-1}^j. \quad (2)$$

which yields

$$R_n^j = \frac{(1 - \mu)P_j}{S_n^j} + \beta = \frac{Z_n^j}{Z_{n-1}^j} \frac{P_j}{S_n^j}. \quad (3)$$

This equation is important as it establishes a relationship between the R_n^j and the parameters of the SIR model. The larger the R_n^j , the larger $\frac{Z_n^j}{Z_{n-1}^j}$ and hence the larger the growth in the number of cases. Given that μ is constant in Equation 3, the larger the infection rate β , the larger the R_n^j . Moreover, the infection rate and thus R_n^j depend on the applied NPIs.

In addition, if we predict the value \hat{R}_n^j , we can also predict the number of cases for day n at GEO j as

$$\hat{X}_n^j = \left(\hat{R}_n^j \frac{S_{n-1}^j}{P_j} - 1 \right) K Z_{n-1}^j + X_{n-K}^j. \quad (4)$$

where K is the size of the temporal window (in days) used to compute the mean number of cases Z_n . As previously explained, in our case $K = 7$ days to mitigate the peculiarities in the reporting schedules of different GEOs and X_n and X_{n-k} are the reported new cases for days n and $n - k$, respectively; \hat{R}_n is the predicted R_n ; P_j is the population of GEO j ; Z_{n-1}^j is the cumulative number of cases the averaged over K days for day $n - 1$ and for GEO j .

The goal of the predictors is to estimate \hat{R}_n^j given the data up to day $n - 1$, similarly as proposed in [7]. Given the dependency of R_n^j on the transmission rate and the dependency of the transmission rate on the NPIs, we describe next predictors that consider both the number of COVID-19 infections (*context*) and the applied NPIs (*actions*) in each GEO and for each day.

C Clustering of countries/regions

In order to build the bank of LSTMs, we clustered the regions using a K-means algorithm applied to the time series of reported number of cases per 100K inhabitants. We used the Elbow method to identify the optimal number of clusters (see Figure 1):

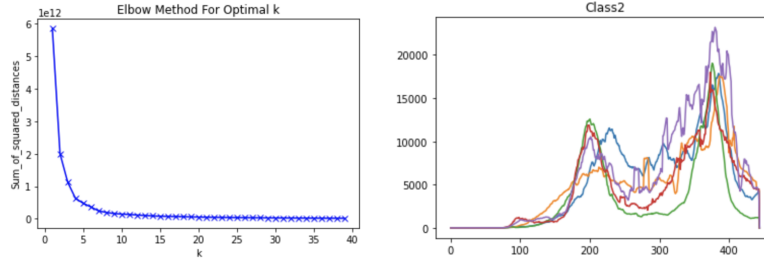


Fig. 1. Left: Selection of 15 clusters via K-means algorithm applied to the time series of reported number of COVID-19 cases. For 15 classes the total squared distance wrt the centers of the clusters is quite stable. Right: Example of one of the classes with the following GEOs: 'Colombia', 'Mexico', 'South Africa', 'Florida' and 'Texas'.

After optimizing the number of clusters, we obtained 15 different clusters (see t-SNE visualization in Figure 2). The Figures below illustrate the clustering of all the GEOs according to the temporal time series of their COVID-19 cases (Figure 3) and the allocation of each GEO to a model in the WT predictor (Figure 4).

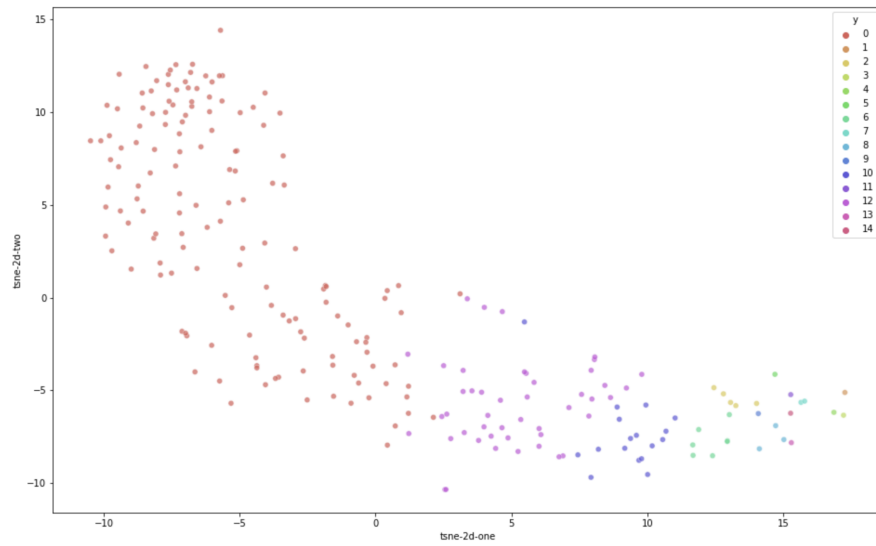


Fig. 2. Clusters and their spatial distribution in a t-SNE visualization.

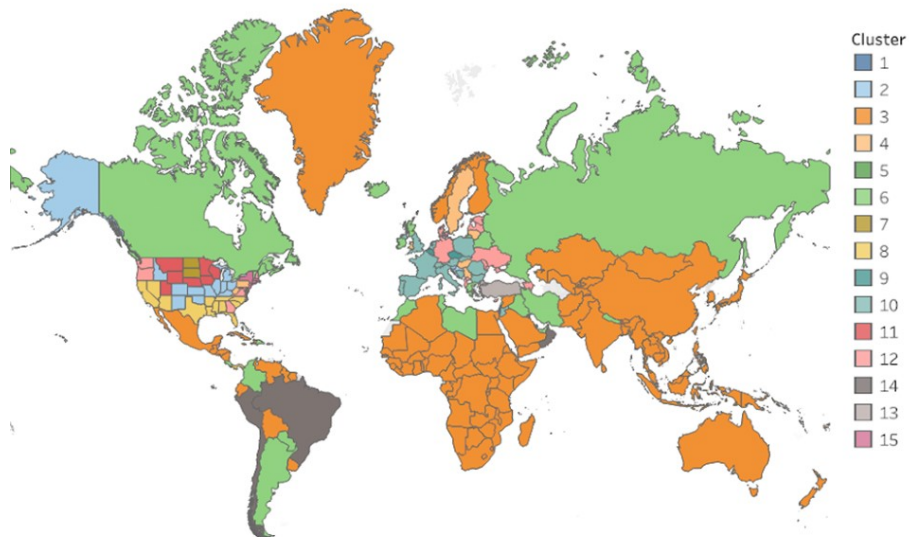


Fig. 3. Clusters obtained by optimizing a K-means algorithm applied to the time series of reported number of COVID-19 cases.

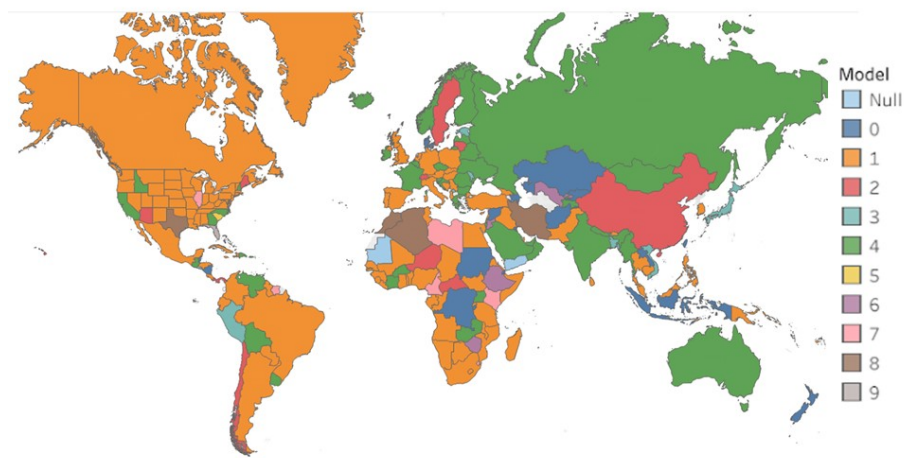


Fig. 4. WT Predictor model allocation, where numbers 0 and 1 correspond to the reference model, and numbers 2 to 9 correspond to the 8 different cluster models that we used in our bank. Note that null is the model we applied in Yemen and Mauritania, which assigns the number of cases based on statistics of the historic data instead of the machine-learning based prediction due to noise in the data.

D Convergence of R_n

D.1 Non-trivial long-term stationary states in epidemiological models

A stationary long-term state which is not the trivial state where all individuals are healthy occurs in several computational epidemiological models. For example, a non-trivial steady state is obtained in simple models derived as the individual mean-field limit of a system describing the spread of a disease in a network when cross-correlations are included (and hence non-linearities) [11,10,5]. Other examples are models obtained as the degree-based mean field limit of a system with house-hold structure [8,6], models that consider the age of the disease [4], etc. Let us detail the first example to motivate our discussion in next section.

Let us consider the spreading of a virus in a graph $G(D, L)$ with D nodes and L links. It is characterized by a symmetric adjacency matrix A . Nodes $\sigma_i(t)$ represent individuals. They can be in state $\sigma_i(t) = 1$ (infected) or $\sigma_i(t) = 0$ (healthy or cured). The infection process is given by a Poisson process with rate β . The recovery process is also a Poisson process, independent from the infection process, with rate γ . The state of the system at time t is thus $\sigma^s(t) = (\sigma_1(t), \sigma_2(t) \dots, \sigma_D(t))$, and there are 2^D possible states, so $s = 0, \dots, 2^D - 1$. Often it is called state of the system to $\sigma(t) = (\sigma^0(t) \dots, \sigma^{2^D-1}(t))$. One can order these states in different ways. A conventional way is to order them as binary numbers (*e.g.*, for $D = 4$, $s = 0$ corresponds to 0000 or $s = 2$ corresponds to 0010). The number of states with c infected nodes is $\binom{D}{c}$.

The dynamics must consider the possible transitions between states $\sigma^s(t)$.

- Recovery dynamics: If individual i is infected, then the transition rate to cured is γ . Given the binary ordering described above, this means that the transition between state s where $\sigma_i(t) = 1$ and state s' where $\sigma_i(t) = 0$, is $q_{ss'} = \gamma$, with $s' = s - 2^{i_1-1}$. For state s this transition occurs for all nodes $\sigma_{i_1}(t)$ which are equal to 1 in state s . Then, here the transition rates $q_{ss'} = \gamma$.
- Contagion dynamics: If individual i is not infected, then it may be infected by all those individuals i' that are connected to it via the adjacency matrix (with elements $a_{ii'}$). The transition rates are β . Here the $s' = s + 2^{i_0+1}$, with i_0 running over all nodes which are in state 0 in state j . Here the transition rates $q_{ss'} = \beta \sum_{k=1}^D \sigma_k(t) a_{i_0 k}$. So node i_0 in state $\sigma^s(t)$ is connected via $a_{i_0 k}$ to the nodes with index k in current state. Those which are 1 may induce infection with rate β . Notice that in the sum all those which are in state 0 (i.e. not infected) do not contribute to the transition rate.

These are the transitions from state s to state s' . Then, in the Master equation these rates multiply the probability of being in state s' . Master equations, as balance equations, must include all transitions from any other state to state s . These multiply vector s so they can be summed up into one coefficient. Therefore,

the Master equation reads

$$\frac{dP(\sigma^s(t))}{dt} = \sum_{s'=s-2^{i_1}-1} q_{ss'} P(\sigma^{s'}(t)) + \sum_{s'=s+2^{i_0}-1} q_{ss'} P(\sigma^{s'}(t)) - \sum_{k=0}^{2^{D-1}} q_{ks} P(\sigma^s(t)).$$

As a matrix, the generator with entries $q_{ss'}$ is a triangular matrix. In the diagonal one finds $q_{ss} = \sum_{k=0}^{2^{D-1}} q_{ks}$. For being a probability, one has to have that $\sum P(\sigma^s(t)) = 1$ as an additional condition.

To compute the probability of node i to be infected, we need to add all the probabilities corresponding to states with the node i equal to $\sigma_i(t) = 1$. That is $P(\sigma_i(t) = 1) = \sum_{s \in \{\bar{X}\}} P(\sigma^s(t))$, where $s \in \{\bar{X}_1\}$ means all those vectors with the condition that at node i they have a 1. Similarly, we proceed for it to be healthy (with $\sigma_i(t) = 0$), here $s \in \{\bar{X}_0\}$ which is the complementary set of $\{\bar{X}_1\}$. This resembles the expectation value of being at value σ_i , with $P(\sigma_i(t) = 1) + P(\sigma_i(t) = 0) = 1$. A quick way to relate the $P(\sigma^s(t))$ states with the $P(\sigma_i(t) = 1)$ is via the M matrix, whose rows are the states in binary representation (which the one we are using), so $P(\sigma_i(t) = 1) = P(\sigma^s(t))M$.

One can write down the generator of the evolution of only these two probabilities, $P(\sigma_i(t) = 1)$ and $P(\sigma_i(t) = 0)$. This is the matrix

$$Q_i = \begin{pmatrix} -q_{1i} & q_{1i} \\ q_{2i} & -q_{2i} \end{pmatrix}.$$

Here $q_{2i} = \gamma$ and $q_{1i} = \sum_{k=1}^D \beta a_{ik} 1_{\sigma_k(t)=1}$, with $1_{\sigma_k(t)=1} = 1$ if $\sigma_k(t) = 1$. To get to the mean field approximation one has to average the Master equation, which gives the equation for the $P(\sigma_i(t) = 1)$ as in the Glauber-Ising dynamics [3]. We call the averages $v_i(t) = P(\sigma_i(t) = 1)$ and the cross correlations $r_{ii'}(t) = P(\sigma_i(t) = 1 | \sigma_{i'}(t) = 1)$. Then we get

$$\frac{dv_i(t)}{dt} = \beta \sum_{k=1}^D a_{ik} v_k(t) - \left(\beta \sum_{k=1}^D a_{ik} r_{ik}(t) + \gamma v_i(t) \right).$$

If we assume independence, i.e. $r_{ii'}(t)$ can be written as $r_{ii'}(t) = P(\sigma_i(t) = 1)P(\sigma_{i'}(t) = 1)$ then this gives a set of non linear equations:

$$\frac{dv_i(t)}{dt} = \beta \sum_{k=1}^D a_{ik} v_k(t) - \left(\beta \sum_{k=1}^D a_{ik} v_k(t) + \gamma \right) v_i(t).$$

The steady state is obtained by making the derivatives equal to zero at infinity (or for $D \gg 1$) $\frac{dv_i(t)}{dt} = 0$. In this model there is a trivial solution in which at the steady state all individuals are healthy. But more importantly, there is a non-trivial solution where the probability of infection of a node at infinite time is non-zero. This solution is enabled by the non-linearity in the equations. This value is expressed $v_i(t \rightarrow \infty) = v_{i,\infty}$. Indeed, as shown in [10], for any effective spreading rate $\tau = \beta/\gamma$ the non-zero steady state for the probability of

node i for being infected is can be expressed as the continued fraction

$$v_{i\infty} = \frac{1}{1 + \tau d_i - \tau \sum_{j=1}^D \frac{a_{ij}}{1 + \tau d_j - \tau \sum_{k=1}^D \frac{a_{jk}}{1 + \tau d_k - \tau \sum_{q=1}^D \frac{a_{kq}}{1 + \tau d_q - \dots}}}},$$

with $d_i = \sum_{j=1}^D a_{ij}$ being the degree (the number of connections) of node i . We make two observations here: i) the stationary state is determined by the parameter τ and the adjacency matrix (which includes the statistics of the network). Note that when an NPI is applied, the network changes, as this is indeed the goal of the measure, *i.e.*, to ideally reduce the connections among individuals so as to minimize the community transmission of the disease. Then, the steady state is different for different NPIs when they are applied over sufficiently long periods of time; ii) The fact that the probability of infection is different from zero means that the total number of infected individuals increases steadily over time, and the number of susceptible individuals decreases.

D.2 Convergence of R_n

Let us briefly give some hints as to why the R_n , as defined in Eq. (3) in the paper, may be expected to converge to a number different than one. In the infinite time limit, the coefficient P^j/S_{n-1}^j is the inverse of the proportion of susceptible individuals in GEO j . According to the aforementioned discussion, this ratio will slightly change over time or be constant, while Z_n^j/Z_{n-1}^j would tend to one. Taking into account the existence of a non-zero steady state which depends on the NPI, as described in Section D, this would imply that R_n^j depends on the implemented NPI, impacting the time series of COVID-19 cases provided that the NPI is applied for long enough. Hence, for sufficiently long time periods, but not in the infinite time limit, we expect the system to reach an equilibrium point. As the system smoothly approaches the equilibrium, Z_n^j/Z_{n-1}^j may be slightly different from one. We conjecture that for large D , that is for large enough networks, all countries which are subject to the same NPI would end up with similar networks. Thus, in the infinite and long-time limits, we would expect a convergence to the same R_n and therefore the convergence behavior would not be an artifact of the predictor but would correspond to an underlying real-world phenomenon. This scaling property, requires a detailed proof that is part of our future work.

E Modeling the $\text{NPI-}\hat{R}_n$ space

Figure 5 (left) depicts the histogram of all possible NPI combinations for each value of stringency with unitary costs. Figure 5 (right) shows the number of combinations for which we computed the convergence R_n .

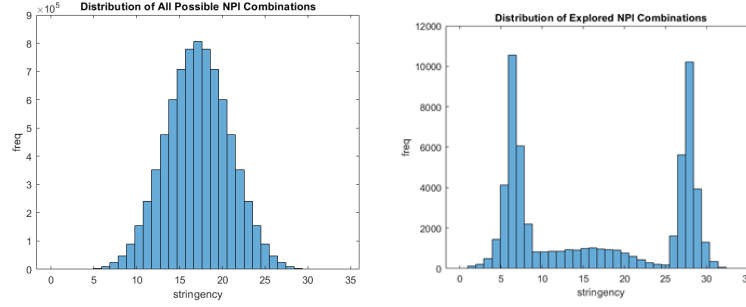


Fig. 5. Left: Histogram of all possible NPI combinations arranged by stringency at unitary costs. Right: Histogram of NPI combinations for which we obtained the $\text{NPI-}R_n$ mapping, by stringency.

Figure 6 shows the feature importance analysis of the 12 different NPIs according to Gradient Boosted Trees.

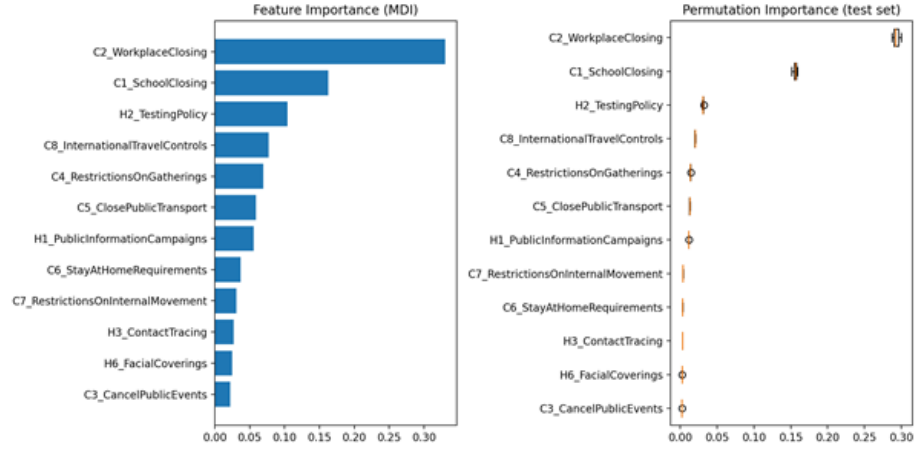


Fig. 6. Feature importance analysis of the NPIs using Gradient Boosted Trees.

F Prescriptor implementation

F.1 Obtaining the Pareto front

Given the input cost vector for a given GEO j ($Cost^j$), and our NPI- \hat{R}_n matrix M , the Pareto front of j is computed at runtime as follows:

1. Apply the input costs to obtain the **stringency** for each NPI combination.
2. Obtain a **feature importance-weighted stringency** vector given by the $Cost^j$ divided by the feature importance of each dimension of the NPI vector.
3. Select a cost column $M_{,cost}$ (the cost may be stringency or feature importance-weighted stringency) and incidence column $M_{,inc}$ (given by the convergence \hat{R}_n or total estimated COVID-19 cases in 20 or 60 days).
4. Sort the matrix of NPIs by $M_{,cost}$ in first place, and $M_{,inc}$ in second place.
5. Create an empty set of selected NPIs in the Pareto front ($selected = \{\}$)
6. For each row i in M , if $M_{i,inc}$ is lower than incidence of the last selected NPI, then add M_i to the *selected* set.

We select the NPIs that are at the intersection of the sets obtained considering both convergence \hat{R}_n and total cases in 20 or 60 days, and stringency and feature importance-weighted stringency as cost and incidence columns respectively.

Figure 7 shows an example visualization of the Pareto front of the NPIs at unitary costs. The color of each dot represents the area in the (cases, stringency)-space of each NPI vector, with the cases normalized as follows

$$cases_N = \frac{cases - \min cases}{\max cases - \min cases}$$

F.2 Selection of NPIs from the Pareto front

Once we have a set of candidates in the Pareto front, the prescriptor selects a maximum of 10 recommended NPIs. In order to keep the most promising NPI combinations, each NPI is assigned a score, obtained as follows. First, the NPI combinations are sorted by cost; next, given the coordinates of NPI i , $c_i = (M_{i,cost}, M_{i,inc})$, the score for NPI i , $score_i$ is computed as:

$$score_i = 1 - \frac{angle(c_{i+1} - c_i, c_{i-1} - c_i) - \frac{\pi}{2}}{\pi}$$

That is, the maximum score is obtained when the angle that forms the NPI vector to the next point wrt the vector of the previous point in the Pareto front is close to $\frac{\pi}{2}$. Conversely, this score is minimum when this angle is close to $\frac{3\pi}{2}$.

All the NPIs whose score is not maximum within a local window in the cost axis are discarded.

F.3 Dynamic Intervention Policy selection

Finally, the prescriptor needs to provide an Intervention Policy, *i.e.* a *dynamic* regime of applying the selected NPIs over the time period of interest. To do

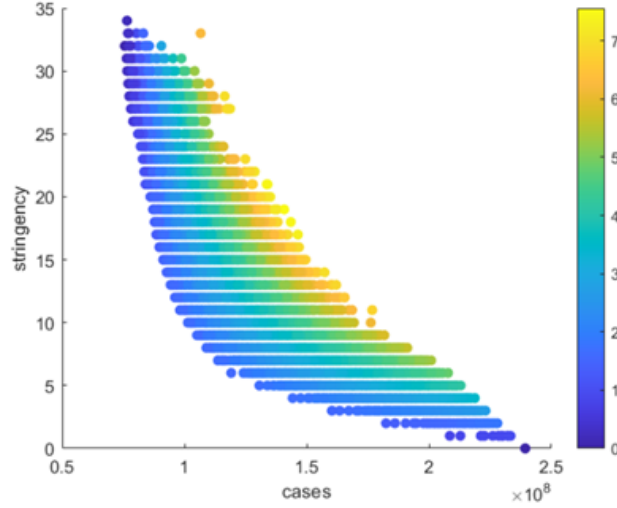


Fig. 7. Exemplary visualization of the Pareto front of NPIs with their associated stringencies at unitary costs.

so, we compute all possible combinations of subsequently applying the selected NPIs in chunks of minimum 14 days (to enable the NPIs to act) and identify the Pareto-front set of combinations that would yield the optimal trade-off between stringency and number of cases. The total number of chunks is dynamically determined, depending on the length of the time period of interest.

Figure 8 depicts an example of such a Pareto front, computed from an initial set of 19 candidate NPIs, *i.e.* the NPIs that are on the Pareto front as per the analysis previously described. In the Figure, the system defines temporal chunks of at least 21 days before changing NPIs and computes the NPI dynamic policy for a period of 60 days. There are 6,859 possible dynamic regimes of applying the NPIs. Of those, 225 (marked in red in the Figure) dominate the rest and constitute a Pareto front of the dynamic NPI policy selection. The color of each dot represents the area in the (cases, stringency)-space of such dynamic NPI combination, normalizing the number of cases as in Figure 7.

From such the set of Intervention Policies on the Pareto front, the prescriptor selects the 10 prescriptions that (1) are not dominated by any other policy; (2) contribute to having a diverse set of policies along the stringency axis and (3) minimize the changes in NPIs, as every NPI change has a social cost from a practical perspective.

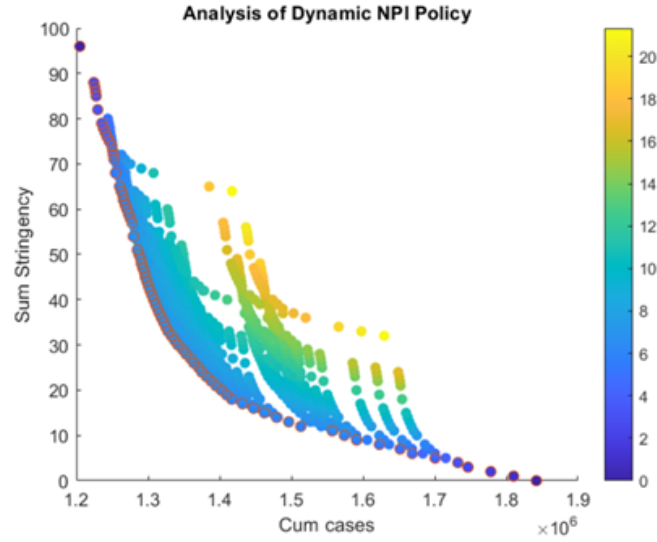


Fig. 8. Example of dynamic Intervention Policy optimization: from 6,859 possible Intervention Policies, 225 are on the Pareto front.

G Prescriptor visualization

Given that the main users of our prescriptor are non-experts (policy-makers, business owners or even citizens), we developed a visualization tool to communicate the ten Intervention Policies (IP) recommended for each GEO and to enable the comparison between two IPs.

The Figures below show a screen shot of the two interfaces of our visualization tool, which can be found here¹.

¹ Anonymized due to double-blind submission.

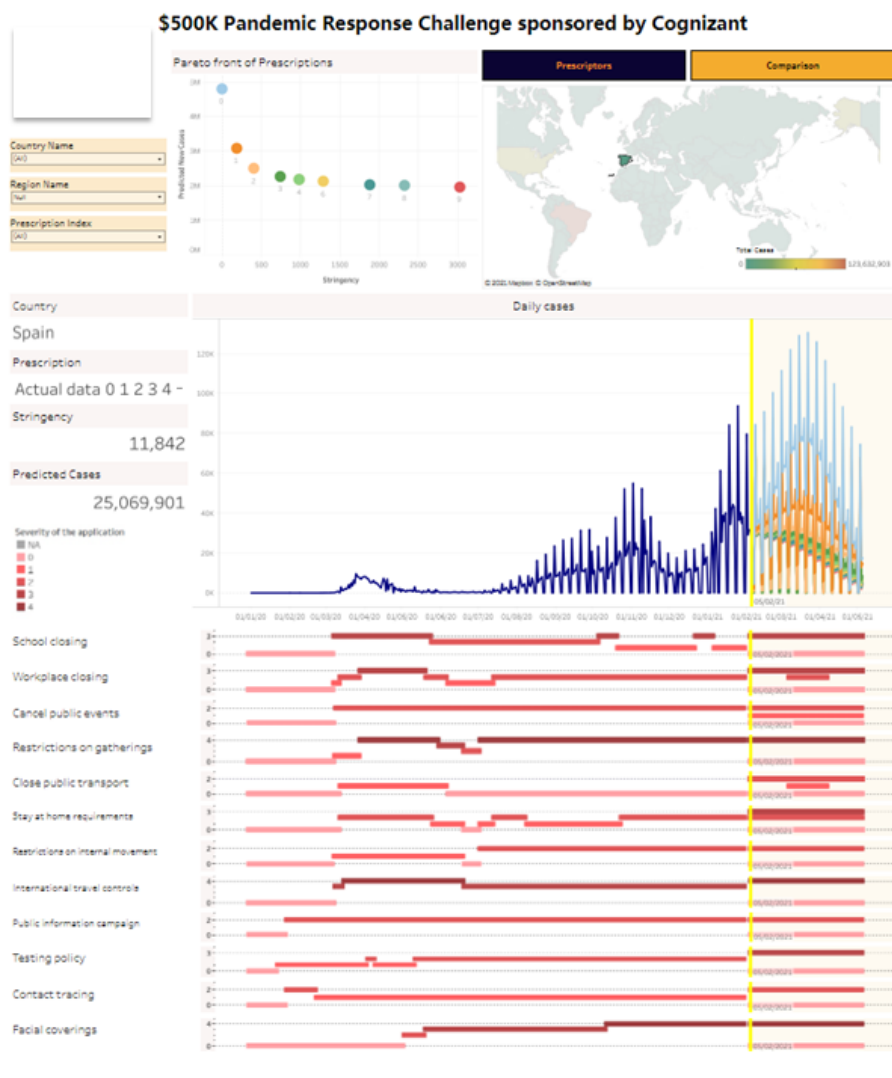


Fig.9. Main window of the visualization tool for the prescriptor. It enables users to select the country/region of interest before it shows the 10 recommended prescriptions with their associated stringencies, total number of predicted COVID-19 cases and levels of activation of each of the 12 dimensions of the NPI vector. It also shows the Pareto front of all prescriptions. In this example, the system shows the 10 selected prescriptions for Spain.

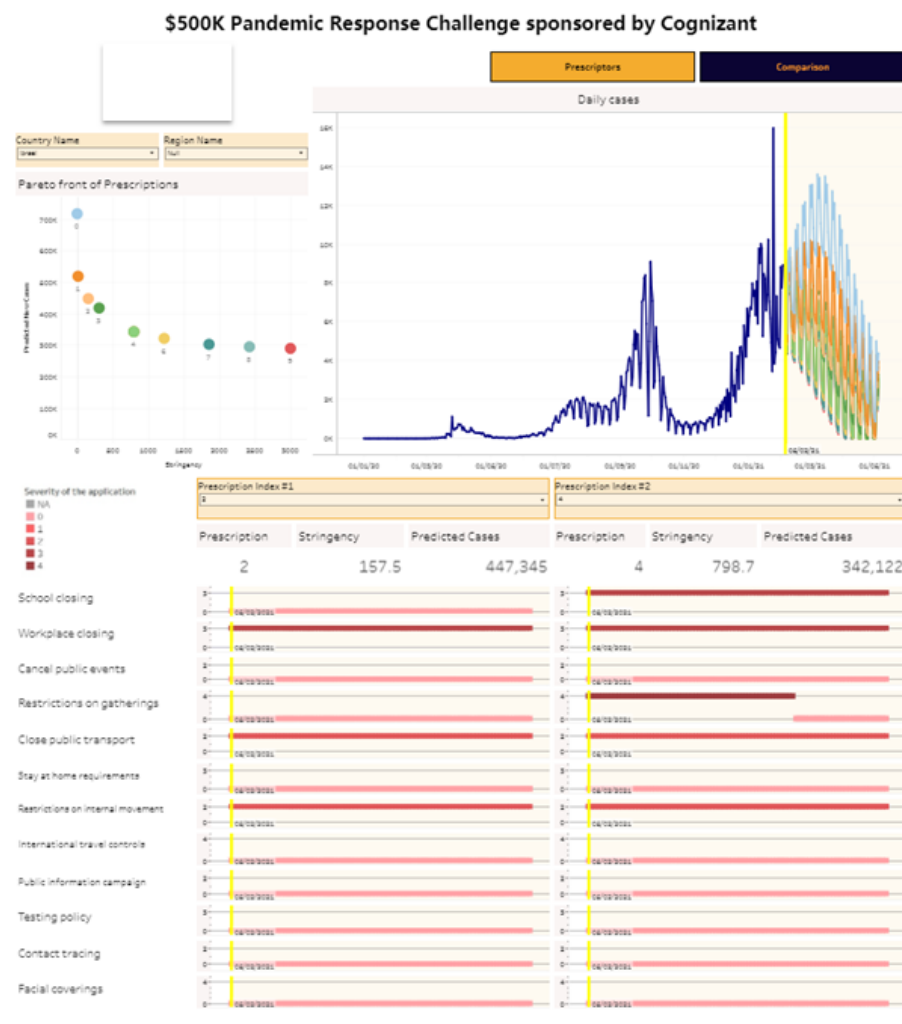


Fig. 10. Secondary window of the visualization tool called "Compare prescriptions". It enables users to select 2 prescriptions of Intervention Policies to compare. In this example, the system shows side to side two prescriptions from the 10 prescriptions proposed for Israel. The prescription on the left (#2) has an overall stringency of 157.5 and would result in 447,345 cases. The prescription on the right (#4) has an overall stringency of 798.7 and would result in 342,122 cases.

References

1. Allen, L.: Some discrete-time SI, SIR, and SIS epidemic models. *Math. Biosci.* **124**(1), 83–105 (1994)
2. Brauer, F., Driessche, P.d., Wu, J.: *Lecture notes in mathematical epidemiology*. Berlin, Germany. Springer **75**(1), 3–22 (2008)
3. Glauber, R.: Time-dependent statistics of the Ising model. *J. Math. Phys.* **4**(2), 294–307 (1963)
4. Inaba, H.: *Age-structured population dynamics in demography and epidemiology*. Springer (2017)
5. Kiss, I., Miller, J., Simon, P., et al.: *Mathematics of epidemics on networks: From exact to approximate models*, *Interdisciplinary Applied Mathematics*, vol. 46. Springer (2017)
6. Liu, J., Wu, J., Yang, Z.: The spread of infectious disease on complex networks with household-structure. *Physica A: Statistical Mechanics and its Applications* **341**, 273–280 (2004)
7. Miikkulainen, R., Francon, O., Meyerson, E., Qiu, X., *et al.*: From prediction to prescription: Evolutionary optimization of nonpharmaceutical interventions in the COVID-19 pandemic. *IEEE Trans. Evol. Comput.* **25**(2), 386–401 (2021)
8. Moreno, Y., Pastor-Satorras, R., Vespignani, A.: Epidemic outbreaks in complex heterogeneous networks. *Eur. Phys. J. B* **26**(4), 521–529 (2002)
9. Rojas, S.: Comment on “estimation of COVID-19 dynamics “on a back-of-envelope”: Does the simplest SIR model provide quantitative parameters and predictions?”. *Chaos, Solitons & Fractals: X* **5**, 100047 (2020)
10. Van Mieghem, P., Omic, J., Kooij, R.: Virus spread in networks. *IEEE/ACM Trans. Netw.* **17**(1), 1–14 (2008)
11. Wang, Y., Chakrabarti, D., Wang, C., Faloutsos, C.: Epidemic spreading in real networks: An eigenvalue viewpoint. In: *22nd International Symposium on Reliable Distributed Systems*, 2003. *Proceedings*. pp. 25–34. IEEE (2003)